La radiologia medica (2019) 124:1049–1061
https://doi.org/10.1007/s11547-019-01060-6

MUSCULOSKELETAL RADIOLOGY

CT and MRI features of scalp lesions

Masaya Kawaguchi[1] · **Hiroki Kato**[1] · **Masayuki Matsuo**[1]

Received: 14 January 2019 / Accepted: 24 June 2019 / Published online: 3 July 2019

Abstract
Scalp lesions can be classified as congenital, traumatic, inflammatory, or neoplastic in origin. Although patients presenting with scalp masses are frequently seen in daily practice, differentiation of scalp lesions is often challenging for radiologists who are not familiar with the imaging of cutaneous lesions. The majority of scalp lesions are fortunately benign, with cystic lesions accounting for over 50% of all benign scalp lesions. Such lesions include trichilemmal cysts (pilar cysts), sebaceoma, epidermoid cysts, dermoid cysts, and teratoid cysts. Radiologists may also occasionally encounter benign neoplasms of the scalp, including melanocytic nevi, keratoacanthoma, pilomatricoma, neurofibroma, and lipoma. Malignant scalp tumors are uncommon; however, they carry a potential risk of delayed detection, resulting in poorer outcomes. Most scalp lesions show nonspecific imaging findings, although some possess characteristic features on CT and MRI. Radiologists must be familiar with the appearances of common scalp lesions to reach an accurate diagnosis. Hence, the aim of this article is to describe the clinical and imaging features of scalp lesions.

Keywords Scalp lesion · Benign · Malignant · CT · MRI

Introduction

Various underlying pathologies exist in patients that present with scalp lesions. It is important that reasonable considerations are made regarding diagnoses before pathological examinations. An accurate interpretation of scalp lesions may allow physicians to appropriately manage different conditions, leading to a reduced mortality and morbidity [1]. In adult populations, 93–98% of all scalp lesions are benign, with the most common diagnosis being trichilemmal cysts (41% of all scalp lesions), followed by epidermal cysts, lipoma, nevi, and sebaceous cysts [2–4]. In pediatric populations, 97–99% of all scalp lesions are benign, with the most common diagnosis being nevus sebaceous (60% of all scalp lesions), followed by infantile hemangioma, melanocytic nevi, and juvenile xanthogranuloma [5, 6]. The scalp is usually described as having five anatomic layers (described in "Anatomy" section) [7]. A clear understanding of the scalp's anatomy is essential for the topographic characterization of the lesion as the first step in the differential diagnosis (Table 1), as the majority (82%) of scalp lesions in adults originate from the skin layer [2].

The rate of correct preoperative diagnosis for scalp lesions ranged from 13 to 27% among neurosurgery, plastic surgery, or general surgery departments [2]. The low diagnostic rate may be caused by a lack of expertise in scalp lesions. Similar to the physicians of these departments, radiologists also encounter scalp lesions during the radiological interpretation for brain CT and MRI in daily practice. However, radiologists are frequently baffled by scalp lesions, because they are not familiar with scalp lesions. Although radiological investigations of some scalp lesions have been reported [8–10], to the best of our knowledge, there have been no review articles with emphasis on CT and MRI features of scalp lesions. Therefore, the aim of this review article is to describe a variety of cutaneous and subcutaneous lesions of the scalp in terms of the anatomic origin with emphasis on CT and MRI features.

Anatomy

The soft-tissue envelope of the cranial vault is named the scalp, extending from the external occipital protuberance and superior nuchal lines to the supraorbital margins and

✉ Hiroki Kato
hkato@gifu-u.ac.jp

[1] Department of Radiology, Gifu University School of Medicine, 1-1 Yanagido, Gifu 501-1194, Japan

Table 1 Classification of scalp lesions

Origin	Benign	Malignant
Keratinocytic origin	Epidermoid cyst/Dermoid cyst/Teratoid cyst, Keratoacanthoma, Seborrheic keratosis	Squamous cell carcinoma, Basal cell carcinoma, Bowen disease
Melanocytic origin	Melanocytic nevus, Blue nevi	Malignant melanoma
Appendageal origin		
Follicular differentiation	Pilomatricoma, Trichilemmal cyst/Proliferating tricholemmal tumor	Pilomatrical carcinoma, Malignant proliferating tricholemmal tumor
Sebaceous differentiation	Sebaceoma/Sebaceous adenoma	Sebaceous carcinoma
Apocrine and eccrine differentiation	Eccrine poroma, Hidrocystoma, Syringoma	Adenocarcinoma, Porocarcinoma, Apocrine carcinoma
Hematolymphoid origin	Langerhans cell histiocytosis, Rosai–Dorfman disease, Juvenile xanthogranuloma	Malignant lymphoma
Soft tissue origin		
Adipocytic	Lipoma, Lipoma variant	Atypical lipomatous tumor, Liposarcoma
Vascular	Infantile hemangioma, Venous malformation/cavernous hemangioma	Angiosarcoma
Lymphatic	Lymphangioma	
Smooth and skeletal muscle	Leiomyoma	Leiomyosarcoma
Fibrous, fibrohistiocytic and histiocytic	Dermatofibroma, Keloid/hypertrophic scar, Infantile myofibromatosis	Dermatofibroma protuberance, Fibrosarcoma
Neural origin	Neurofibroma, Schwannoma	Merkel cell carcinoma, Malignant peripheral nerve sheath tumor
Others	Dermoid/teratoid cyst	Metastasis

anchored laterally by each ear. The scalp consists of five histologic layers: skin, subcutaneous tissue (superficial fascia), galea aponeurotica (deep fascia), loose areolar connective tissue, and pericranium (Fig. 1) [1, 3, 7]. The first three layers are bound together into a single unit. This single unit can move along the loose areolar tissue over the pericranium adherent to the calvaria.

The skin is the outermost region of the scalp, which is composed of thin external epidermis and thick inner dermis, which both decrease in thickness with age. The epidermis is composed of stratified squamous epithelium, with a thickness of 0.04–0.4 mm. The dermis is usually thinnest over the forehead and thickest over the occipital region [1, 3] with a thickness of 0.5–2.5 mm. The skin also contains closely arranged adnexa (consisting of sebaceous glands, hair follicles, and eccrine and apocrine glands) surrounded by dense networks of blood vessels and lymphatics [3].

The subcutaneous tissue, also known as the subcutis or superficial fascia, is a fibrofatty layer that connects the skin to the underlying galea aponeurotica of the occipitofrontalis muscle and provides a passageway for blood vessels, nerves, and lymphatic tissue. At the vertex, the subcutaneous tissue has a thickness of 4–7 mm.

The galea aponeurotica, also called the deep fascia, is a strong, thin, tendinous sheath that descends laterally into the temporal fossa as the superficial temporal fascia. This layer splits anteriorly into superficial and deep layers, to envelop the frontalis and the orbicularis muscle. The galea aponeurotica has a thickness of 1–2 mm.

The loose connective tissue, which is also referred to as the areolar tissue, comprises the subgaleal layer between the galea aponeurotica and the pericranium. This layer contains the most widely distributed connective tissues and is composed of a central dense collagenous layer surrounded by vascularized areolar tissue. This layer has several functions, including support and binding, fluid retention, defense, and nutrient storage.

The periosteum covering the outer surface of the skull is known as the pericranium. The pericranium is a fibrous membrane that is tightly attached to the outer table of the skull. Laterally, it terminates at the origin of the temporalis muscle along the superior temporal line.

Imaging

The skin layer presents on CT as a soft-tissue density and on MRI as isointense to muscle. This layer shows enhancement on contrast-enhanced images because of the rich vascular network derived from the subcutaneous layer. However, the dermis and the epidermis are indistinguishable from one another on these images. Upon encountering cutaneous lesions arising from the skin layer, the depth of the lesion

and the invasion of nearby subcutaneous tissue should be assessed by radiologists on the basis of CT and MRI.

The subcutaneous tissue layer appears as a hypodense area on CT and as an area with hyperintensity on T1- and T2-weighted MR images because of its fat content. On fat-suppressed contrast-enhanced T1-weighted images, the enhancement of subcutaneous tissue can be observed because of its rich vascular network.

The galea aponeurotica layer is shown on MRI as an area that is isointense to muscles. In contrast, the loose connective tissue and the pericranium cannot normally be visualized by either CT or MRI and can only be detected pathologically [7].

The depth of tumor invasion is an important prognostic factor for local recurrence and distant metastasis after surgery. If cutaneous lesions invade the subcutaneous tissue, the subcutaneous tissue appears as an area of hyperintensity on fat-suppressed T2-weighted images and as an area of hypointensity on T1-weighted images. In many cases, however, abnormal intensities of subcutaneous tissue on MRI actually reflect inflammatory cell infiltration rather than tumor invasion. As a result, radiologists often tend to overdiagnose the depth of invasion. Therefore, an accurate depth of invasion should be confirmed during the assessment of resected specimens. The depth of scalp invasion, from skin toward the dura, can be classified into three categories, each requiring different extents and techniques of surgical resection.

1. Superficial type. The tumor lies superficial to the galea aponeurotica; resection can be carried out to the level of the galea aponeurotica.
2. Intermediate type. The tumor has penetrated the galea aponeurotica; satisfactory oncological resection implies the inclusion of the periosteum into the surgical specimen. The outer table of the cranium can be included if the periosteum is involved in the lesion.
3. Deep type. The tumor extends down to the cranial bone; full-depth resection is required, including the dura if necessary.

Benign lesions

Trichilemmal cysts, proliferating trichilemmal tumors

Trichilemmal cysts, otherwise known as pilar cysts or isthmus-catagen cysts, are the most common form of intradermal or subcutaneous cysts of the scalp, accounting for 5–10% of the population. Despite their high frequency, most cases might be mistakenly misdiagnosed owing to the lack of recognition. These cysts arise preferentially in areas with dense concentrations of hair follicles; 90% of the cases occur in the scalp [11]. Cases usually occur in middle-aged subjects, with a female predilection. Histologically, these cysts are lined by squamous epithelium, containing a granular layer (trichilemmal keratinization) that is filled with homogenous keratin. Calcifications are common features in trichilemmal cysts. In 2% of the cases, proliferating cells in single or multiple foci grow into proliferating trichilemmal tumors [11]. Although proliferating trichilemmal tumors are generally considered benign, there have been reports of malignant transformation.

On CT, trichilemmal cysts appear as well-defined, hypodense masses with occasional focal calcification (Fig. 2). On T1-weighted images, homogeneous isointensity to the brain parenchyma is considered pathognomonic for trichilemmal cysts, compared with hypointensity of epidermoid cysts [12]. The presence of calcification causes inhomogeneity on T2-weighted images; the lack of intralesional enhancement can be observed on contrast-enhanced images (Fig. 2) [12]. Proliferating trichilemmal tumors show heterogeneous signal intensities on T2-weighted images (Fig. 3). On contrast-enhanced T1-weighted images, these tumors show significant enhancement of walls, with variable thicknesses and mural nodules. These factors reflect the pathological components of solid lobules and cystic cavities [13]. As the underlying skull vault and skin surface are not affected by trichilemmal cysts, enhanced soft-tissue components with irregular margins, invasion into surrounding structures, and erosion of adjacent bony tissue are indicative signs of malignant transformation.

Sebaceoma

Sebaceous neoplasms are uncommon cutaneous tumors arising in the sebaceous glands, which are responsible for secreting lipids and other substances into the hair follicle infundibulum [14]. Sebaceous neoplasms comprise a spectrum ranging from benign to malignant, including hyperplasia,

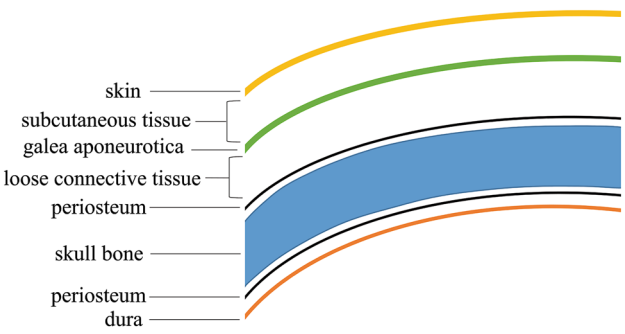

Fig. 1 Schema of the scalp. The scalp consists of five histologic layers: skin, subcutaneous tissue (superficial fascia), galea aponeurotica (deep fascia), loose connective tissue, and periosteum (pericranium)

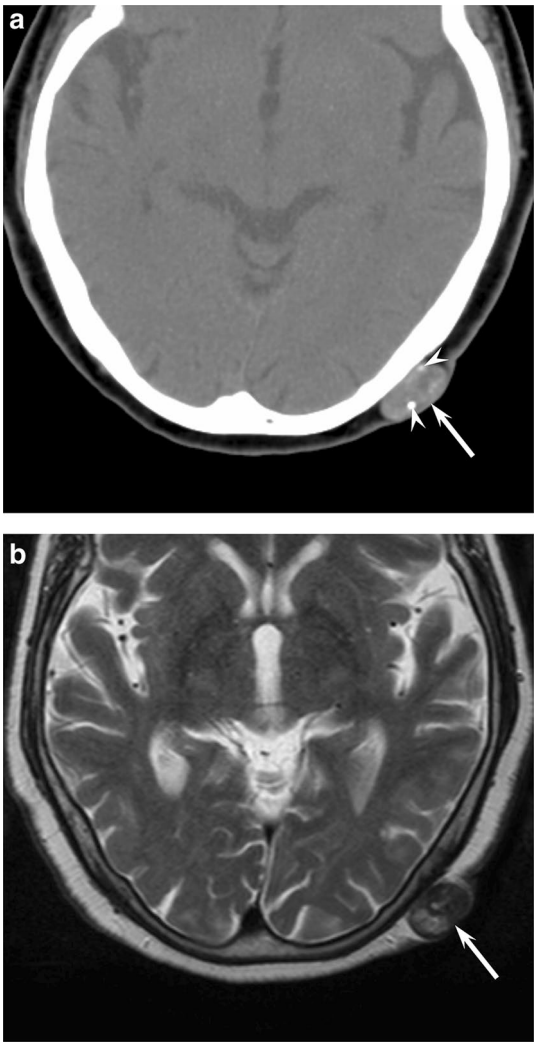

Fig. 2 A 75-year-old woman with trichilemmal cyst. **a**. Unenhanced CT image shows a well-demarcated subcutaneous lesion (arrow) with calcification (arrow heads). **b**. T2-weighted image shows heterogeneously low to high signal intensity (arrow)

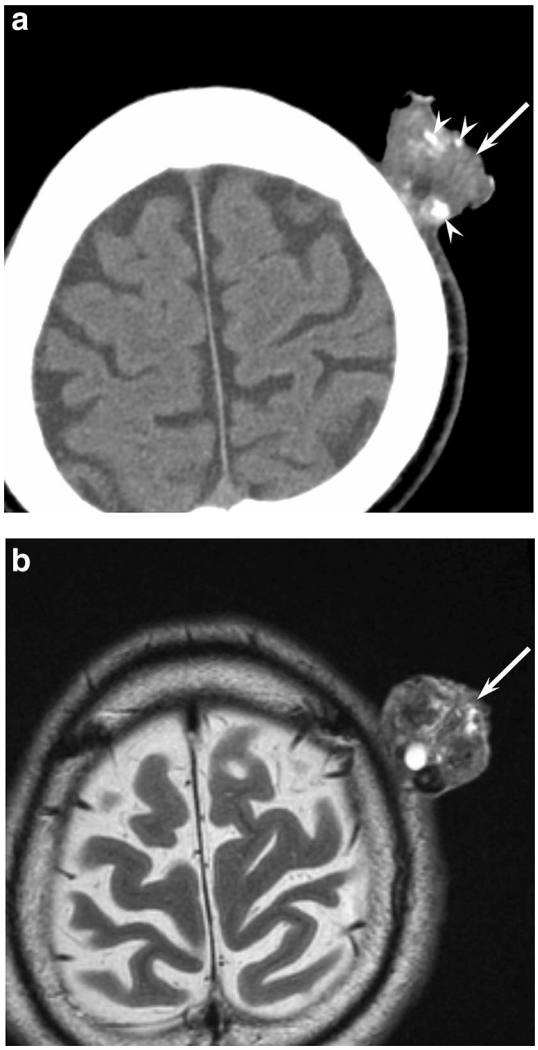

Fig. 3 A 62-year-old man with proliferating trichilemmal tumor. **a** Unenhanced CT image shows a irregular-shaped lesion (arrow) with calcification (arrow heads). **b** T2-weighted image shows heterogeneously low to high signal intensity (arrow)

adenoma, sebaceoma, and carcinoma. Sebaceomas range from 5 to 30 mm in maximum diameter, typically occurring on the face and the scalp. Sebaceomas tend to occur in the sixth decade and beyond, with a female predilection [14, 15]. Histologically, sebaceomas are located in the mid dermis, containing a clear oily liquid, small amounts of keratinous material, and lanugo hair [16]. The cystic wall is lined by stratified squamous epithelium, with sebaceous lobules present in, or adjacent to, the cystic wall.

Sebaceomas are located in the dermis and frequently expand downward to the subcutaneous tissue layer [16]. On CT and MRI, sebaceomas present as well-defined, encapsulated cystic masses. If abundant oil content is present within sebaceomas, they appear as areas of hyperintensity on T1- and T2-weighted images (Fig. 4). In contrast, if the cystic cavities are filled with large amounts of keratin and hair, they appear as areas with hypo- to isointensity on T1-weighted images and hyperintensity on T2-weighed images.

Epidermoid/dermoid/teratoid cysts

Epidermoid, dermoid, and teratoid cysts are common, related, cutaneous cysts lined by squamous epithelium, classified according to whether they are lined by simple squamous epithelium (epidermoid cysts), the presence of skin adnexa in the cystic wall (dermoid cysts), or the presence of other tissues, such as muscle, cartilage, or bone (teratoid cysts). Such cysts are derived from the epidermis and form through cystic enclosure of the epithelium within the dermis, which is filled with keratin and lipid-rich debris. These types

of cysts occur in the head and neck region, generally occurring in young to middle-aged adults with a male-to-female ratio of 3:1. Dermoid and teratoid cysts are usually found as congenital masses in pediatric patients [17].

On CT and MRI, these types of cysts appear as well-demarcated, oval-shaped, subcutaneous cystic masses adjacent to the overlying skin. Epidermoid cysts appear as areas with iso- to hyperintensity on T1-weighted images and hyperintensity with variable hypointense foci, including internal linear dark debris, on T2-weighted images (Fig. 5) [10]. Although peripheral, thin-rim enhancement without central enhancement is usually observed, the rupture of epidermoid cysts results in the enhancement of internal septa and a thickened, irregular rim, with fuzzy enhancement in surrounding subcutaneous tissues [18]. Dermoid cysts typically appear as areas with hyperintensity due to their fat content on T1-weighted images and variable intensities on T2-weighted images [19]. Teratoid cysts show as the presence of calcification on CT, reflecting the formation of cartilage or bone.

Keratoacanthoma

Keratoacanthoma is a self-limiting, epidermal tumor that is cryptic because of its nosological position at the border between benignity and malignancy [20]. Keratoacanthoma is usually solitary, with a clinical history of rapid growth over four to 5 weeks and spontaneous regression after 6 months [21]. This condition generally occurs on sun-exposed skin (e.g., face and arms) during the fifth to seventh decades. Lesions are usually 1–2 cm in diameter, typically showing an exophytic–endophytic architecture with a central keratotic horn and overhanging epithelial lips [21]. Although its pathological features are remarkably similar to those of squamous cell carcinoma (SCC), keratoacanthoma is characterized by a rapid growth, symmetrical structure, and non-invasive nature.

On CT and MRI, keratoacanthomas appear as exophytic, dome- or cup-shaped, well-demarcated cutaneous nodules with central recesses of keratotic horns (Fig. 6). Circularly symmetrical configurations accompanied by sharp boundaries with deeper subcutaneous tissue can be observed. Lesions show an intermediate intensity on T1-weighted images and a mixture of intermediate and high signal intensities on T2-weighted images with peripheral thin-rim enhancement [22].

Pilomatricoma

Pilomatricoma, which is also known as calcifying epithelioma, is a rare, benign tumor of the dermis or subcutaneous tissue, which originates from pluripotent cells that normally differentiate into hair matrix cells [8]. Pilomatricoma occurs

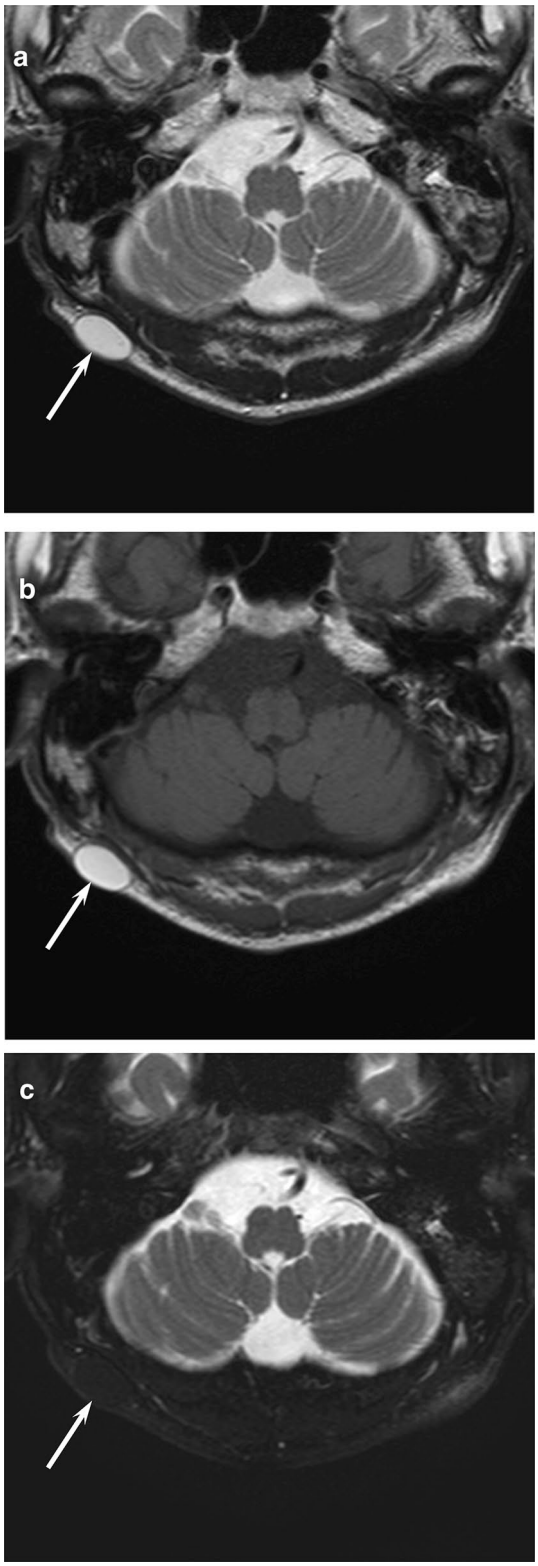

Fig. 4 A 66-year-old man with sebaceoma. **a** T2-weighted image shows a well-demarcated, homogeneously hyperintense, subcutaneous lesion (arrow). **b** T1-weighted image shows homogeneous hyperintensity (arrow). **c**. Fat-suppressed T2-weighted image shows decreased signal intensity (arrow)

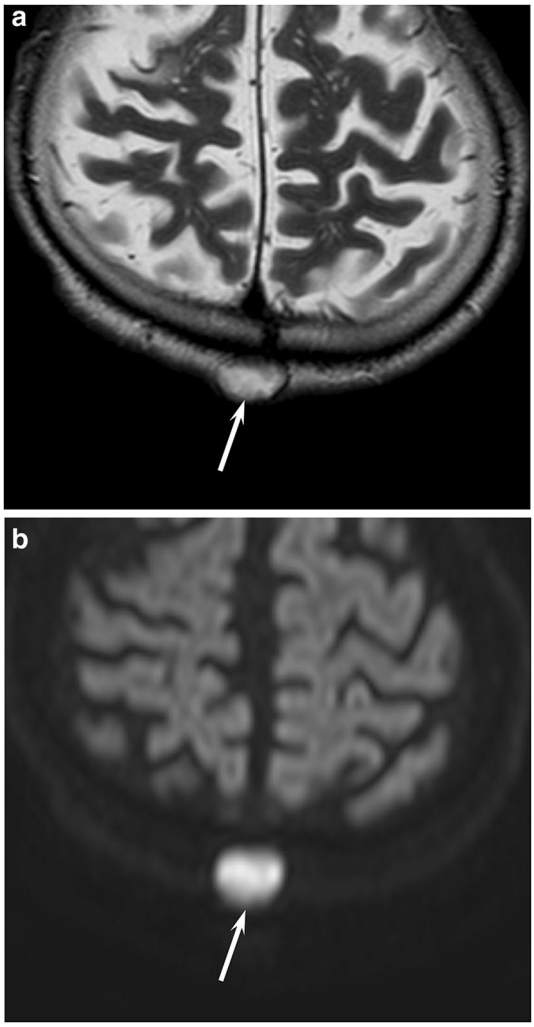

Fig. 5 A 56-year-old man with epidermoid cyst. **a** T2-weighted image shows a well-demarcated, heterogeneously hyperintense, subcutaneous lesion (arrow). **b** Diffusion-weighted image shows intense hyperintensity (arrow)

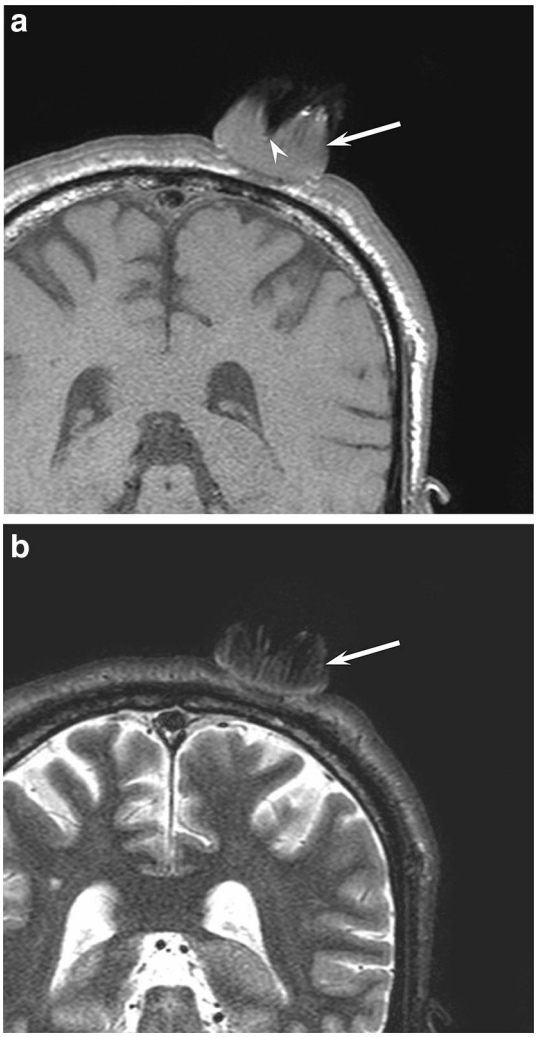

Fig. 6 A 51-year-old man with keratoacanthoma. **a** T1-weighted image shows a exophytic, cup-shaped, well-demarcated cutaneous lesion (arrow) with central recesses of keratotic horn (arrow head). **b** Fat-suppressed T2-weighted image shows heterogeneous iso- to hypointensity (arrow)

over a wide age range, most commonly (approximately in 60% of the cases) in the first and second decades, with a male-to-female ratio of 1:1.1 [23]. Approximately, half of the tumors occur in the head and neck region, followed by the upper extremities, trunk, and lower extremities; the sites that are most commonly affected by pilomatricoma are the cheek, neck, eyebrows, and scalp [23]. Histologically, pilomatricoma appears as epithelial cell islands composed of basaloid cells and shadow cells, surrounded by edematous and fibrous stroma [8].

On CT, pilomatricomas present as well-demarcated, subcutaneous masses with various levels of calcification (Fig. 7). Reticular and ring-like hyperintensities on fat-suppressed T2-weighted and fat-suppressed contrast-enhanced T1-weighted images are frequently observed, corresponding to intratumoral stroma and tumor capsule with various degrees of inflammatory cell infiltration and vascular proliferation, respectively (Fig. 7) [8]. Inflammatory cell infiltration into peritumoral fat occasionally causes peritumoral fat stranding on fat-suppressed T2-weighted images [8].

Melanocytic nevi

Melanocytic nevi, which is also called moles, are common skin lesions that are characterized by benign clonal proliferation of cells expressing a melanocytic phenotype, with heterogeneous clinical and molecular characteristics [24]. Melanocytic nevi are formed by nests of melanocytes in epidermal junctions (junctional nevi), dermis (intradermal nevi), or both compartments (compound nevi). Their peak incidence is in the fourth to fifth decades, with a female

Fig. 7 A 4-year-old girl with pilomatricoma. **a** Unenhanced CT image shows a well-demarcated subcutaneous lesion (arrow) with faint calcification (arrow heads). **b** T2-weighted image shows heterogeneously low to high signal intensity (arrow). **c** Fat-suppressed contrast-enhanced T1-weighted image shows reticular and ring-like enhancement (arrow) with perilesional fat stranding (arrow heads)

predilection. Congenital nevi of the scalp tend to lighten over time and thus become cosmetically less bothersome [3]. As the risk of malignant transformation of melanocytic nevi strongly depends on size, giant congenital melanocytic nevi are associated with an increased risk of malignant melanoma.

Melanocytic nevi present as flat patch lesions on the skin. Hyperdensity relative to soft tissue has been observed on CT owing to the melanin content of melanocytic nevi. The paramagnetic effect of intralesional melanin deposition results in iso- to hyperintensity on T1-weighted images and hypointensity on T2-weighted images (Fig. 8). Although melanocytic nevi rarely invade the underlying fascia, muscle, or deeper structures, giant congenital melanocytic nevi may invade the subcutaneous tissue or beyond with ill-defined margins.

Neurofibroma

Neurofibroma is a benign nerve sheath tumor with a neuroectodermal origin, accounting for 5% of all benign soft-tissue tumors [25]. Based on the histology, neurofibroma can be classified into three categories: localized, plexiform, and diffuse types. Localized neurofibroma is the most common, accounting for approximately 90% of all cases [25]. Plexiform neurofibroma involves extensive nerve segments and branches, often extending beyond the epineurium into the surrounding tissue. Diffuse neurofibroma is an uncommon form that generally occurs among children and young adults, typically in the head and neck region. At least 10% of diffuse neurofibromas are associated with neurofibromatosis type 1.

Diffuse neurofibroma involves both the skin and the subcutaneous tissue, also frequently extending to the fascia over muscle, commonly with plaque-like or infiltrative growth patterns. Plaque-like growth appears as thick slabs of abnormal tissue with no interposed noninvolved tissue, with a mean plaque thickness of 2.5 cm (Fig. 9) [25]. Infiltrative growth shows poorly demarcated masses with interposed uninvolved tissue [25]. Despite being mildly or markedly hyperintense to muscle in T2-weighted images and isointense or mildly hyperintense to muscle in T1-weighted images, MR signal intensities of neurofibroma are typically nonspecific [25].

Vascular anomalies/Infantile hemangioma

Vascular anomalies can be divided into two main categories: vascular tumors and malformations. Vascular tumors comprise infantile hemangioma, congenital hemangioma, and kaposiform hemangioendothelioma. Infantile hemangiomas are the most common childhood tumors, with an incidence of 12–23% among low-birth-weight, preterm infants and with a female-to-male ratio of 3:1 [26]. Hemangiomas

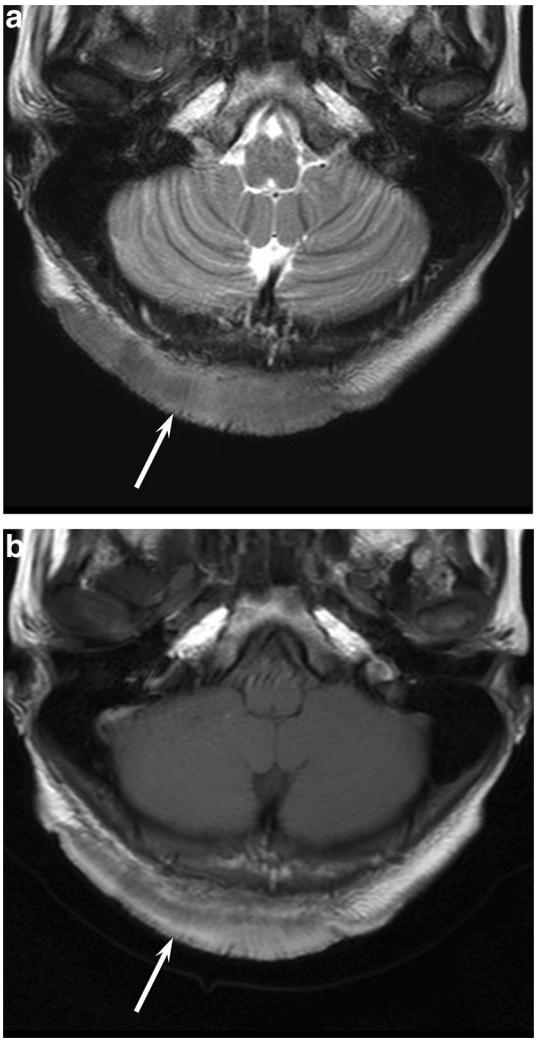

Fig. 8 A 20-year-old woman with melanocytic nevi. **a** T2-weighted image shows an ill-demarcated, heterogeneously hypo- to hyperintense, subcutaneous lesion (arrow). **b** T1-weighted image shows heterogeneous iso- to hyperintensity (arrow)

frequently occur in the head and neck region (60% of the cases), typically presenting two to 6 weeks after birth as small lesions and rapidly growing in the first 12–18 months (proliferating phase). Subsequently, half of all the cases are completely resolved by 5 years of age (involuting phase).

Infantile hemangiomas typically appear as well-defined, lobulated, noninfiltrating masses, with hypointensity on T1-weighted images and hyperintensity on T2-weighted images (Fig. 10) [27, 28]. Fast-flow vessels are identified by the presence of flow voids within and around soft-tissue masses [28]. On contrast-enhanced T1-weighted images, homogeneous, early intense enhancement in the proliferating phase and decreased enhancement in the involuting phase are observed. Perilesional edema is not generally observed in infantile hemangioma (Fig. 10).

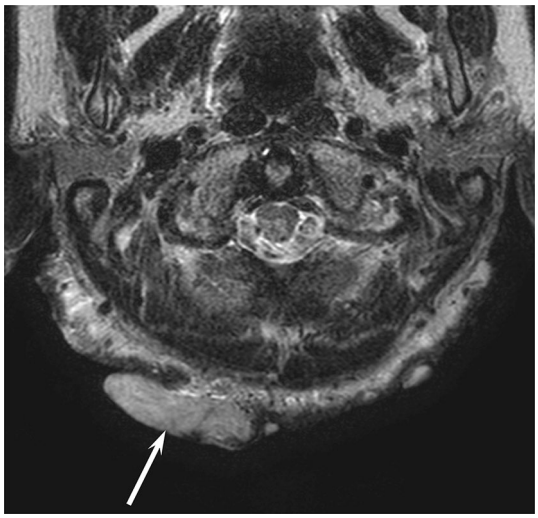

Fig. 9 A 61-year-old woman with diffuse neurofibroma associated with neurofibromatosis type 1. T2-weighted image shows a heterogeneously hyperintense lesion with plaque-like growth (arrow)

Lipoma

Lipoma is the most common type of benign mesenchymal tumor, which is composed of mature fat cells. As lipomas of the scalp frequently occur on the forehead, these lesions are also referred to as frontalis-associated lipoma [29, 30]. Based on the location relative to the fascia overlying the deep muscles, lipomas are categorized as superficial or deep. Deep lipomas account for 60–64% of all forehead lipomas, significantly greater than the frequency of deep lipomas occurring in other sites (0.4–6%) [29]. Surgical approaches and planning differ between superficial and deep lipomas; therefore, accurate assessment of localization is necessary for radiologists.

On CT, lipomas appear as round or ovoid, well-delineated homogeneous masses associated with fat attenuation. MRI is useful for demonstrating the presence of fat signal intensity [1]. On fat-suppressed images, noticeable reductions in the lesion signal intensity are depicted. The findings of a large tumor size, thick septa with moderate or marked enhancement, and nodular or patchy nonadipose components are indicative of well-differentiated liposarcomas [31].

Malignant tumors

Basal cell carcinoma (BCC) and Squamous cell carcinoma (SCC)

BCC and SCC are the most common histologic subtypes of malignant cutaneous tumors of the scalp, accounting for 41% and 17% of all cases, respectively [32]. Overall, 2–18%

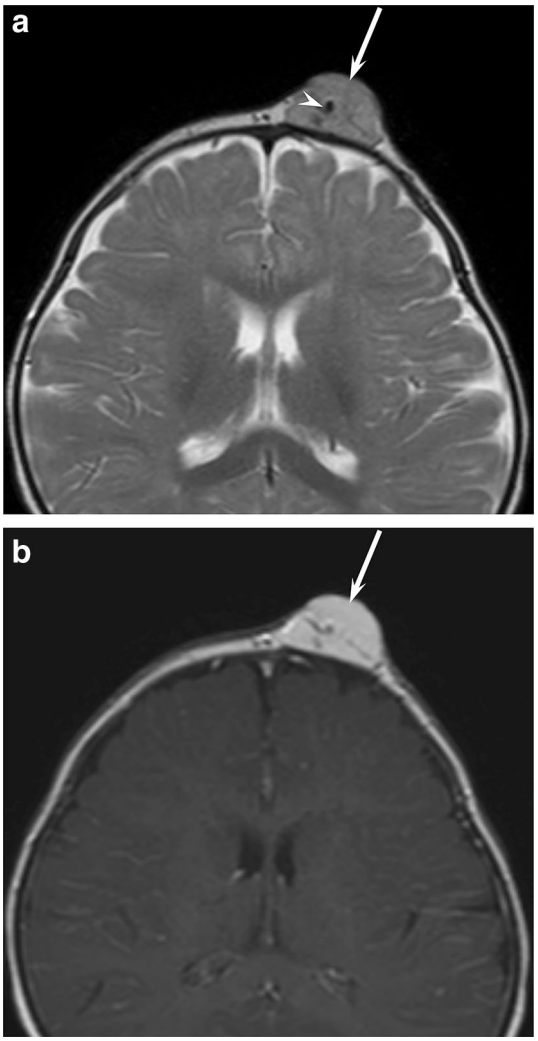

Fig. 10 A 9-month-old boy with infantile hemangioma. **a** T2-weighted image shows a well-demarcated, heterogeneously hyperintense, subcutaneous lesion (arrow) with flow void (arrow head). **b** Fat-suppressed contrast-enhanced T1-weighted image shows homogeneously intense enhancement (arrow)

of BCCs and 3–8% of SCCs are located on the scalp [3]. BCCs and SCCs of the scalp usually occur in patients in the sixth to seventh decades, with a female-to-male ratio of 1.1:1 and 1.3:1 for BCCs and SCCs, respectively [32]. BCCs and SCCs of the scalp have a greater tendency to ulcerate, compared with other locations on the skin. As SCCs of the scalp are often diagnosed at an advanced stage, this location may be considered an independent risk factor for poor prognosis [3]. BCCs of the scalp recur frequently, but rarely infiltrate the cranium and dura [3]. For SCCs and BCCs of the scalp, the maximum diameter greater than 10 mm, the poorly defined borders, the recurrent tumor, and the history of immunosuppression and prior radiation therapy are clinical manifestations indicative of high-risk tumors.

BCCs and SCCs usually appear as flat lesions, occasionally accompanied by central recesses. As BCCs and SCCs both show nonspecific hypointensity on T1-weighted images and iso- to hyperintensity on T2-weighted images (Fig. 11) [33], BCCs and SCCs are indistinguishable from one another with MRI. SCCs are more likely to be invasive than BCCs; however, peritumoral or deeper soft-tissue enhancement may be seen more often in cases of SCCs than in those of BCCs on contrast-enhanced T1-weighted images.

Malignant melanoma

Malignant melanoma is a malignancy of pigment-producing cells (melanocytes), which are located predominantly in the skin. Head and neck melanomas comprise 18% of all melanomas, and 7% of all melanomas arise on the scalp [34]. Melanomas of the scalp frequently occur in the sixth decade, with a male predilection (male-to-female ratio = 4:1), which is significantly greater than for other sites [34]. The tumor thickness of melanomas is greater in the scalp (2.6 mm) than in other sites (1.7–1.9 mm), correlating positively with the risk of lymph node and distant metastasis. The location of melanoma on the scalp is, therefore, an independent adverse prognostic factor [34].

Stable-free radicals within melanin pigments are paramagnetic and induce shortening of T1 and T2 relaxation times; therefore, the expected signal pattern for melanotic melanoma is hyperintensity on T1-weighted images and hypointensity on T2-weighted images (Fig. 12) [33]. In contrast, amelanotic melanomas show hypo- to isointensity to the cortex on T1-weighted images and hyper- to isointensity on T2-weighted images [33]. The signal intensity varies depending on several factors, and intralesional hemorrhage also has a significant effect on MRI.

Merkel cell carcinoma (MCC)

MCC is a rare, aggressive, primary cutaneous neuroendocrine carcinoma. It typically occurs in elderly, fair-skinned individuals in the seventh and eighth decades, with a slight male predilection. As sun exposure is considered a significant risk factor for MCC (81%), cases frequently occur in the head and neck region, accounting for 29–48% of all primary MCCs [35]. MCCs grow rapidly, with a propensity for local recurrence and regional lymph node metastasis; large MCCs of the scalp carry a high risk of distant metastasis [36].

MCCs present as nodules in the skin and subcutaneous layer (Fig. 13), generally measuring between 1.0 and 1.5 cm, with slight hyperintensity to muscle on T1-weighted images and hyperintensity on T2-weighted images. Subcutaneous reticular stranding and satellite nodules are characteristic of MCCs, due to peritumoral lymphatic spread with lymphangitis carcinomatosa and lymphatic metastasis [9]. Significant

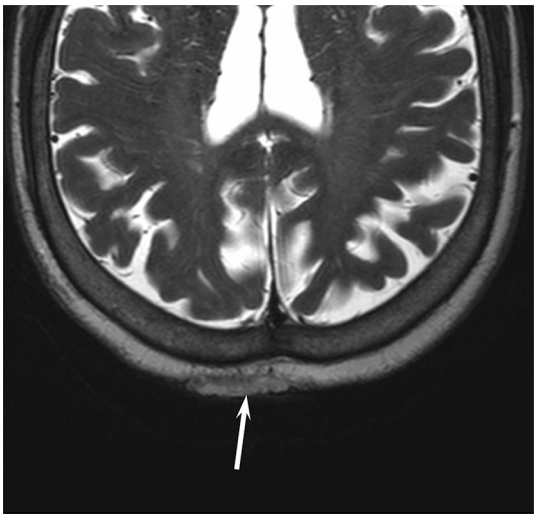

Fig. 11 A 76-year-old woman with basal cell carcinoma. T2-weighted image shows an ill-demarcated, heterogeneously isointense, cutaneous lesion (arrow)

lymph node enlargement is often observed, alongside fine, compressed, retained fatty tissue [9].

Angiosarcoma

Angiosarcoma is a malignant tumor of vascular endothelial cells, often associated with local recurrence and metastasis, resulting in a poor prognosis. Angiosarcomas represent < 1% of all soft-tissue sarcomas, and their most frequent sites are the skin and subcutis. Cutaneous angiosarcomas are most common in patients aged ≥ 70, with a male predilection. Angiosarcomas of the head and neck region account for 60% of all cases [37] and are usually found on the scalp and face. The proposed risk factors for angiosarcoma include prior radiation exposure, chronic lymphoedema, and exposure to chemicals [37].

Angiosarcomas generally show nonspecific isointensity to muscle on T1-weighted images and hyperintensity on T2-weighted images (Fig. 14). Hyperintense areas on T1-weighted images indicate the presence of intratumoral hemorrhage. The characteristic findings for angiosarcoma include the presence of high-flow serpentine vessels, whereas low-flow vessels may show hyperintensity on T2-weighted images [37]. On contrast-enhanced images, solid components are intensely enhanced, whereas tumor necrosis is depicted as nonenhancing areas [37].

Metastasis

Cutaneous metastasis from primary visceral malignancy is clinically relatively uncommon, with a reported incidence

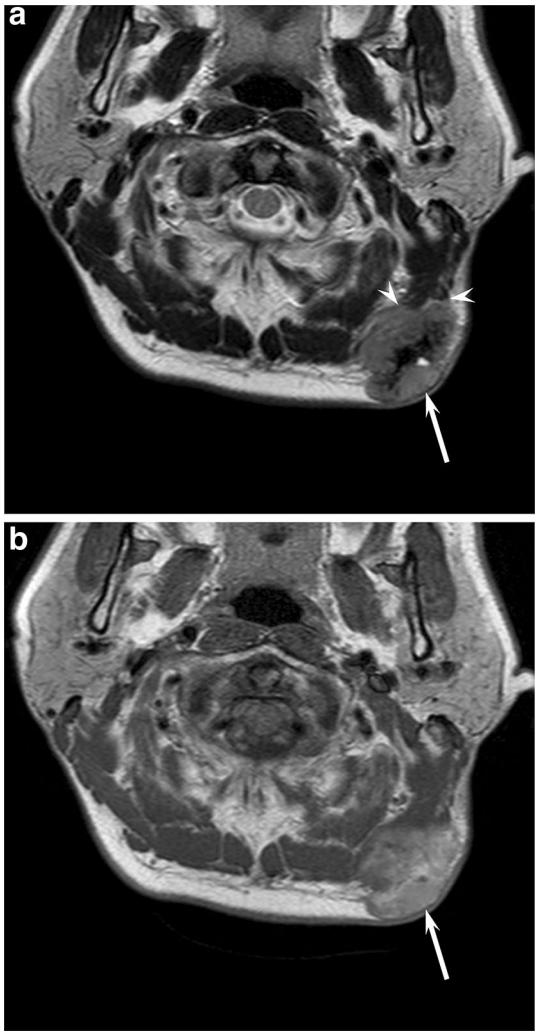

Fig. 12 A 52-year-old man with malignant melanoma. **a** T2-weighted image shows a heterogeneously hypo- to isointense, subcutaneous lesion (arrow) with muscular invasion (arrow heads). **b** T1-weighted image shows heterogeneous hyperintensity (arrow)

ranging from 0.22 to 10%, whereas 40% of the cases with cutaneous metastases also present with internal metastases [38]. Scalp metastases account for 4–7% of all cutaneous metastases. The scalp is potentially a relatively frequent metastatic site because of its abundant blood supply, immobility, and warmth [39]. Scalp metastasis is associated with various primary sites, including the lungs, breast, and stomach, and frequently occurs in older patients, with a mean age of 50 years.

Imaging findings depend on the histologic features of the primary tumor (Fig. 15). On CT and MRI, cutaneous and subcutaneous metastases commonly manifest as multiple, variable-sized, poorly defined nodules, or as infiltrative soft-tissue masses with homogeneous or heterogeneous contrast enhancement.

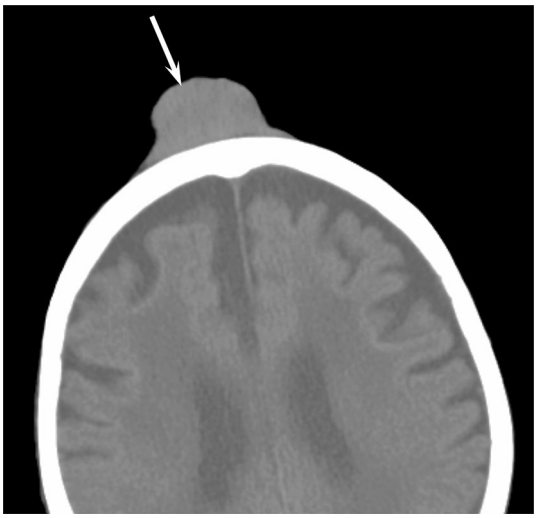

Fig. 13 A 98-year-old woman with merkel cell carcinoma. Unenhanced CT image shows a homogeneous soft-tissue lesion (arrow)

Malignant lymphoma

Malignant lymphoma accounts for 0.6–4.8% of all malignant scalp tumors [2, 32]. Although the skin is the second most common site for extranodal non-Hodgkin's lymphoma, lymphoma of the scalp is rare [3]. In most cases, lymphoma of the scalp occurs in the cranial vault and subsequently infiltrates the adjacent subcutaneous tissue, accompanied by systemic or cerebral parenchymal involvement. The most common B-cell lymphomas of the scalp are primary cutaneous follicle center lymphoma and primary cutaneous marginal zone lymphoma, both of which have excellent prognoses [3]. Among T-cell lymphomas, mycosis fungoides is the most common subtype, which occurs on the scalp [3]. Scalp lymphomas occur across a wide range of ages, with a mean age of 46 years, with no gender predilection [32].

Cutaneous lymphomas appear as areas of isointensity on T1- and T2-weighted images because of their high cellularity (Fig. 16). On diffusion-weighted images, restricted diffusion with significantly low apparent diffusion coefficient values is observed. Tumor margins tend to have a thorny appearance, extending into the subcutaneous tissue, suggestive of lymphatic spread [33]. If lymphomas present with subcutaneous bulky masses of the scalp with extensive cranial vault involvement, both bone lymphoma with scalp invasion and cutaneous lymphoma with bone invasion should be considered as differential diagnoses.

Conclusions

Although CT and MRI play important roles in tissue characterization and evaluating the depth of invasion of scalp lesions, it is challenging for radiologists to differentiate between scalp tumors because the imaging findings are typically similar and nonspecific. To enable an accurate differentiation of scalp tumors, theoretical speculation throughout the diagnostic process is required, based on the scalp's anatomy. Therefore, it is essential for radiologists to be familiar with the scalp's anatomy and the imaging features of scalp lesions.

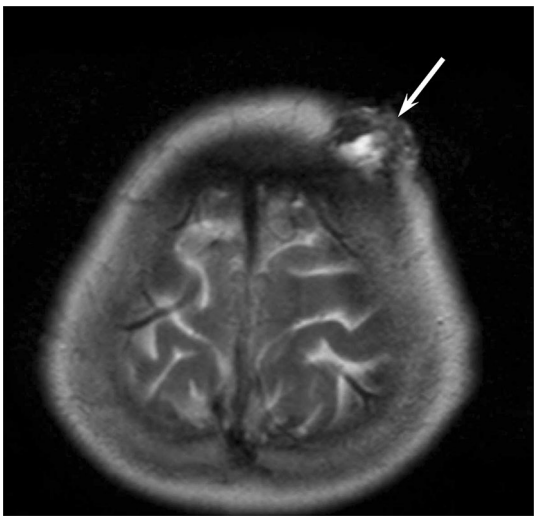

Fig. 14 A 88-year-old man with angiosarcoma. T2-weighted image shows a heterogeneously hypo- to hyperintense lesion (arrow)

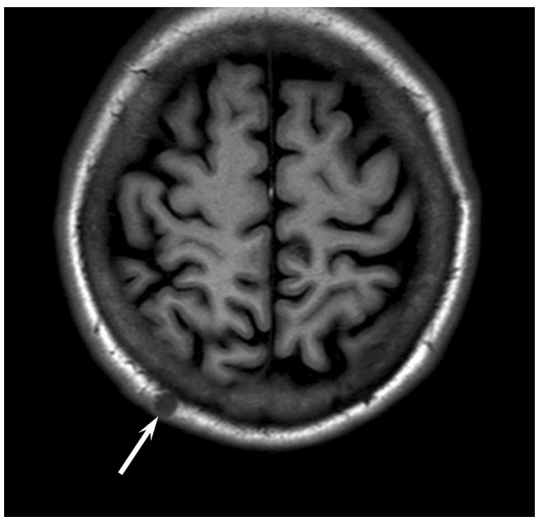

Fig. 15 A 62-year-old woman with metastasis from renal cell carcinoma. T1-weighted image shows a hypointense subcutaneous nodule (arrow)

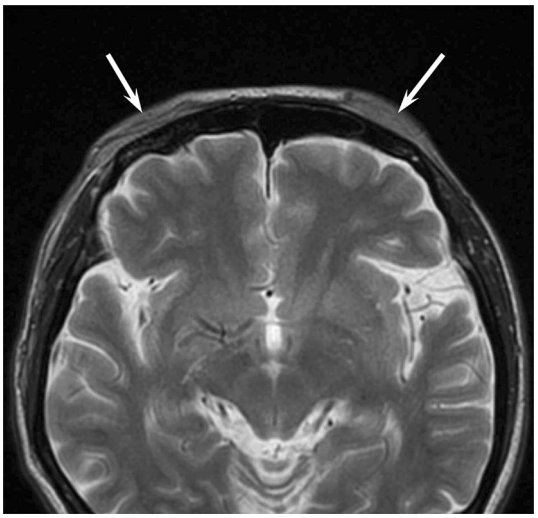

Fig. 16 A 52-year-old woman with mucosa-associated lymphoid tissue lymphoma. T2-weighted image shows a homogeneously isointense subcutaneous lesions (arrows)

Compliance with ethical standards

Conflict of interest The authors declare that they have no conflict of interest.

Ethical approval All procedures performed in studies involving human participants were in accordance with the ethical standards of the institutional and/or national research committee and with the 1964 Helsinki Declaration and its later amendments or comparable ethical standards. For this type of study, formal consent is not required.

Human and animal rights This article does not contain any studies with human participants performed by any of the authors.

Informed consent For this type of study, formal consent is not required. The requirement for informed consent was waived due to the retrospective nature of this study.

References

1. Morcillo Carratala R, Capilla Cabezuelo ME, Herrera Herrera I, Calvo Azabarte P, Dieguez Tapias S, Moreno de la Presa R, Aragon Tejada FX (2017) Nontraumatic lesions of the scalp: practical approach to imaging diagnosis: neurologic/head and neck imaging. Radiographics 37(3):999–1000. https://doi.org/10.1148/rg.2017160112
2. Turk CC, Bacanli A, Kara NN (2015) Incidence and clinical significance of lesions presenting as a scalp mass in adult patients. Acta Neurochir (Wien) 157(2):217–223. https://doi.org/10.1007/s00701-014-2266-7
3. Prodinger CM, Koller J, Laimer M (2018) Scalp tumors. J Dtsch Dermatol Ges 16(6):730–753. https://doi.org/10.1111/ddg.13546
4. Garcia-Rojo B, Garcia-Solano J, Sanchez-Sanchez C, Montalban-Romero S, Martinez-Parra D, Perez-Guillermo M (2001) On the utility of fine-needle aspiration in the diagnosis of primary scalp lesions. Diagn Cytopathol 24(2):104–111
5. Yang CC, Chen YA, Tsai YL, Shih IH, Chen W (2014) Neoplastic skin lesions of the scalp in children: a retrospective study of 265 cases in Taiwan. Eur J Dermatol 24(1):70–75. https://doi.org/10.1684/ejd.2013.2216
6. Yoon SH, Park SH (2008) A study of 77 cases of surgically excised scalp and skull masses in pediatric patients. Childs Nerv Syst 24(4):459–465. https://doi.org/10.1007/s00381-007-0523-2
7. Sharman AM, Kirmi O, Anslow P (2009) Imaging of the skin, subcutis, and galea aponeurotica. Semin Ultrasound CT MR 30(6):452–464
8. Kato H, Kanematsu M, Watanabe H, Nagano A, Shu E, Seishima M, Miyazaki T (2016) MR imaging findings of pilomatricomas: a radiological-pathological correlation. Acta Radiol 57(6):726–732. https://doi.org/10.1177/0284185115597717
9. Anderson SE, Beer KT, Banic A, Steinbach LS, Martin M, Friedrich EE, Stauffer E, Vock P, Greiner RH (2005) MRI of merkel cell carcinoma: histologic correlation and review of the literature. AJR Am J Roentgenol 185(6):1441–1448. https://doi.org/10.2214/AJR.04.0796
10. Kim HK, Kim SM, Lee SH, Racadio JM, Shin MJ (2011) Subcutaneous epidermal inclusion cysts: ultrasound (US) and MR imaging findings. Skeletal Radiol 40(11):1415–1419. https://doi.org/10.1007/s00256-010-1072-4
11. Ramaswamy AS, Manjunatha HK, Sunilkumar B, Arunkumar SP (2013) Morphological spectrum of pilar cysts. N Am J Med Sci 5(2):124–128. https://doi.org/10.4103/1947-2714.107532
12. Gossner J, Larsen J (2010) Incidental subcutaneous nodules on the scalp in patients undergoing CT of the brain; frequency, appearance, and differential diagnosis. Clin Radiol 65(5):427–428. https://doi.org/10.1016/j.crad.2010.01.006
13. Kitajima K, Imanaka K, Hashimoto K, Hayashi M, Kuwata Y, Sugimura K (2005) Magnetic resonance imaging findings of proliferating trichilemmal tumor. Neuroradiology 47(6):406–410. https://doi.org/10.1007/s00234-004-1328-6
14. Lazar AJ, Lyle S, Calonje E (2007) Sebaceous neoplasia and Torre-Muir syndrome. Curr Diagn Pathol 13(4):301–319. https://doi.org/10.1016/j.cdip.2007.05.001
15. Shalin SC, Lyle S, Calonje E, Lazar AJ (2010) Sebaceous neoplasia and the Muir-Torre syndrome: important connections with clinical implications. Histopathology 56(1):133–147. https://doi.org/10.1111/j.1365-2559.2009.03454.x
16. Park KY, Oh KK, Noh TW (2003) Steatocystoma multiplex: mammographic and sonographic manifestations. AJR Am J Roentgenol 180(1):271–274. https://doi.org/10.2214/ajr.180.1.1800271
17. Prior A, Anania P, Pacetti M, Secci F, Ravegnani M, Pavanello M, Piatelli G, Cama A, Consales A (2018) Dermoid and epidermoid cysts of scalp: case series of 234 consecutive patients. World Neurosurg 120:119–124. https://doi.org/10.1016/j.wneu.2018.08.197
18. Hong SH, Chung HW, Choi JY, Koh YH, Choi JA, Kang HS (2006) MRI findings of subcutaneous epidermal cysts: emphasis on the presence of rupture. AJR Am J Roentgenol 186(4):961–966. https://doi.org/10.2214/AJR.05.0044
19. Sorenson EP, Powel JE, Rozzelle CJ, Tubbs RS, Loukas M (2013) Scalp dermoids: a review of their anatomy, diagnosis, and treatment. Childs Nerv Syst 29(3):375–380. https://doi.org/10.1007/s00381-012-1946-y
20. Kwiek B, Schwartz RA (2016) Keratoacanthoma (KA): an update and review. J Am Acad Dermatol 74(6):1220–1233. https://doi.org/10.1016/j.jaad.2015.11.033
21. Ko CJ (2010) Keratoacanthoma: facts and controversies. Clin Dermatol 28(3):254–261. https://doi.org/10.1016/j.clindermatol.2009.06.010
22. Choi JH, Shin DH, Shin DS, Cho KH (2007) Subungual keratoacanthoma: ultrasound and magnetic resonance imaging findings.

Skeletal Radiol 36(8):769–772. https://doi.org/10.1007/s00256-007-0274-x
23. O'Connor N, Patel M, Umar T, Macpherson DW, Ethunandan M (2011) Head and neck pilomatricoma: an analysis of 201 cases. Br J Oral Maxillofac Surg 49(5):354–358. https://doi.org/10.1016/j.bjoms.2010.06.002
24. Viana AC, Gontijo B, Bittencourt FV (2013) Giant congenital melanocytic nevus. An Bras Dermatol 88(6):863–878. https://doi.org/10.1590/abd1806-4841.20132233
25. Hassell DS, Bancroft LW, Kransdorf MJ, Peterson JJ, Berquist TH, Murphey MD, Fanburg-Smith JC (2008) Imaging appearance of diffuse neurofibroma. AJR Am J Roentgenol 190(3):582–588. https://doi.org/10.2214/AJR.07.2589
26. Bhat V, Salins PC, Bhat V (2014) Imaging spectrum of hemangioma and vascular malformations of the head and neck in children and adolescents. J Clin Imaging Sci 4:31. https://doi.org/10.4103/2156-7514.135179
27. Flors L, Leiva-Salinas C, Maged IM, Norton PT, Matsumoto AH, Angle JF, Hugo Bonatti M, Park AW, Ahmad EA, Bozlar U, Housseini AM, Huerta TE, Hagspiel KD (2011) MR imaging of soft-tissue vascular malformations: diagnosis, classification, and therapy follow-up. Radiographics 31(5):1321–1340. https://doi.org/10.1148/rg.315105213 **(discussion 1340–1321)**
28. Dubois J, Alison M (2010) Vascular anomalies: what a radiologist needs to know. Pediatr Radiol 40(6):895–905. https://doi.org/10.1007/s00247-010-1621-y
29. Lee JS, Hwang SM, Jung YH, Kim HI, Kim HD, Hwang MK, Kim MW (2014) Clinical Characteristics of the Forehead Lipoma. Arch Craniofac Surg 15(3):117–120. https://doi.org/10.7181/acfs.2014.15.3.117
30. Sewell LD, Adams DC, Marks VJ (2008) Subcutaneous forehead nodules: attention to the button osteoma and frontalis-associated lipoma. Dermatol Surg 34(6):791–798. https://doi.org/10.1111/j.1524-4725.2008.34148.x
31. Ohguri T, Aoki T, Hisaoka M, Watanabe H, Nakamura K, Hashimoto H, Nakamura T, Nakata H (2003) Differential diagnosis of benign peripheral lipoma from well-differentiated liposarcoma on MR imaging: is comparison of margins and internal characteristics useful? AJR Am J Roentgenol 180(6):1689–1694. https://doi.org/10.2214/ajr.180.6.1801689
32. Chiu CS, Lin CY, Kuo TT, Kuan YZ, Chen MJ, Ho HC, Yang LC, Chen CH, Shih IH, Hong HS, Chuang YH (2007) Malignant cutaneous tumors of the scalp: a study of demographic characteristics and histologic distributions of 398 Taiwanese patients. J Am Acad Dermatol 56(3):448–452. https://doi.org/10.1016/j.jaad.2006.08.060
33. Kim JH, Kim JY, Chun KA, Jee WH, Sung MS (2008) MR imaging manifestations of skin tumors. Eur Radiol 18(11):2652–2661. https://doi.org/10.1007/s00330-008-1015-9
34. Ozao-Choy J, Nelson DW, Hiles J, Stern S, Yoon JL, Sim MS, Faries MB (2017) The prognostic importance of scalp location in primary head and neck melanoma. J Surg Oncol 116(3):337–343. https://doi.org/10.1002/jso.24679
35. Bichakjian CK, Olencki T, Aasi SZ, Alam M, Andersen JS, Blitzblau R, Bowen GM, Contreras CM, Daniels GA, Decker R, Farma JM, Fisher K, Gastman B, Ghosh K, Grekin RC, Grossman K, Ho AL, Lewis KD, Loss M, Lydiatt DD, Messina J, Nehal KS, Nghiem P, Puzanov I, Schmults CD, Shaha AR, Thomas V, Xu YG, Zic JA, Hoffmann KG, Engh AM (2018) Merkel cell carcinoma, Version 1.2018, NCCN clinical practice guidelines in oncology. J Natl Compr Canc Netw 16(6):742–774. https://doi.org/10.6004/jnccn.2018.0055
36. Smith VA, Camp ER, Lentsch EJ (2012) Merkel cell carcinoma: identification of prognostic factors unique to tumors located in the head and neck based on analysis of SEER data. Laryngoscope 122(6):1283–1290. https://doi.org/10.1002/lary.23222
37. Gaballah AH, Jensen CT, Palmquist S, Pickhardt PJ, Duran A, Broering G, Elsayes KM (2017) Angiosarcoma: clinical and imaging features from head to toe. Br J Radiol 90(1075):20170039. https://doi.org/10.1259/bjr.20170039
38. Gul U, Kilic A, Gonul M, Kulcu Cakmak S, Erinckan C (2007) Spectrum of cutaneous metastases in 1287 cases of internal malignancies: a study from Turkey. Acta Derm Venereol 87(2):160–162. https://doi.org/10.2340/00015555-0199
39. Salemis NS, Veloudis G, Spiliopoulos K, Nakos G, Vrizidis N, Gourgiotis S (2014) Scalp metastasis as the first sign of small-cell lung cancer: management and literature review. Int Surg 99(4):325–329. https://doi.org/10.9738/INTSURG-D-13-00070.1